Fault-Induced Transient Analysis for Real-Time Fault Detection and Location in Transmission Lines

F. B. Costa* and B. A. Souza**

Abstract—**The real-time detection of the fault-induced transients on both transmission line terminals can allow the directional protection system to detect and locate faults in agreement with a high-speed fault clearance. This paper presents a wavelet-based method for real-time detection of the fault-induced transients. The method can detect whether the fault is within the protected line and estimate the fault location through a communication link at both line terminals. The wavelet coefficients were computed with both the Discrete Wavelet Transform (DWT) and the Maximal Overlap Discrete Wavelet Transform (MODWT). However, the MODWT provided faster fault detection and better fault location. The method was implemented and evaluated by means of the Real Time Digital Simulator (RTDS).**

Index Terms—**Fault-induced transients, fault location, transmission line protection, real-time wavelet transform.**

I. Introduction

HIGH-SPEED fault detection and location are important issues in power system engineering in order to clear the faults quickly, restoring power supply as soon as possible with minimum interruption. In this context, the traveling wave-based protection can provide very fast relay operation in transmission lines. However, the high-frequency components of the traveling waves generated by the system faults are not within conventional transducer bandwidths. On the other hand, the traveling wave detection requires a high sampling frequency, limiting its application. To overcome these drawbacks, the fault-induced transients with a typical frequency spectrum from a few hundred Hz to various kHz can provide extensive information about the fault type, detection, location, direction, and sustained time in satisfactory agreement with real application in high-speed protective relays [1], [2], [3].

Fault-induced transients are non-stationary in both time and frequency domains. In this way, voltages and currents with fault-induced transients can be properly analyzed by using the DWT. This transformation is a well-known powerful tool to detect transients in power system disturbances [4], [5], such as fault-induced transients in three-phase overhead transmission lines. Much research has been focused on wavelet-based techniques applied on analyzing power system transients [6], [7], [8], detecting and classifying faults [9], [10], and estimating the fault location [11], [12].

This work was supported by the Brazilian National Research Council (CNPq) and PROPESQ-UFRN.

*The author is with Federal University of Rio Grande do Norte - School of Science and Technology, Campus Univesitário Lagoa Nova, Natal - RN, CEP:59.078-970, Brazil. E-mail: flaviocosta@ect.ufrn.br.

**The author is with the Department of Electrical Engineering at Federal University of Campina Grande, 882 Aprígio Veloso Av, Bodocongó, Campina Grande - PB, CEP:58.109-970, Brazil. E-mail: benemar@ee.ufcg.edu.br.

Presented at the International Conference on Power Systems Transients (IPST'11) in Delft, Netherlands on June 14-17, 2011.

The fault-induced transients can be detected in real-time by means of the wavelet coefficient analysis [13]. The energies of the wavelet coefficients have also been used to detect and classify faults in real-time [14]. The real-time analysis of the wavelet coefficients can lead to the development of worthy fault detection and location methods to yield results in satisfactory agreement with real protective applications. Notwithstanding, the number of published papers regarding the real-time fault detection and location methods based on wavelet transforms has been small.

The MODWT is a variant of the DWT which does not use the down-sampling process. In real-time applications, the wavelet coefficients of the MODWT are computed in each simulation time step or soon after each sampling process. As a consequence, the fault-induced transients can be detected faster by using the MODWT [13].

This paper addresses a fault detection and location method based on the real-time analysis of the wavelet coefficients. The proposed method is composed by three modules: 1) real-time detection of the fault-induced transients by using the wavelet coefficients of both the phase voltages and currents just at local terminal; 2) Identification of internal or external faults upon the protected line by using wavelet information from both terminals; 3) real-time fault location estimation by using wavelet information from both terminals.

The RTDS was used in order to evaluate the performance of the proposed fault detection and location method. The wavelet coefficients at first scale of both the MODWT and DWT were used for fault-induced transient detection, and good results were obtained. However, as expected, the fault-induced transients were detected faster and the estimation of the fault location was better with the MODWT-based method.

II. Preprocessing of the Real-Time Fault Detection and Location

Fig. 1 depicts a simplified flowchart of the proposed real-time fault location method. The voltages and currents are obtained from the system through potential transformers (PTs) and current transformers (CTs), respectively. Anti-aliasing filters with an appropriate cut frequency followed by analog to digital converters are required to convert the signals into digital signals. In this paper, the wavelet coefficients of the sampled voltages and currents are computed in real-time. These coefficients are used by the proposed method in order to detect and locate faults in real-time. The process to compute the real-time wavelet coefficients are described in the remainder of this section, and the real-time fault detection and location is properly addressed in the next section.

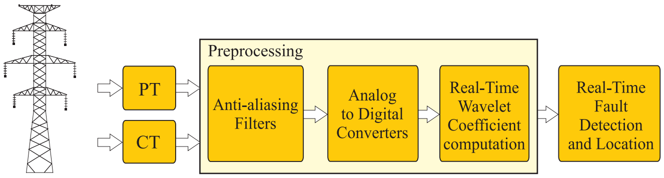

Fig. 1. Flowcharting of the preprocessing module.

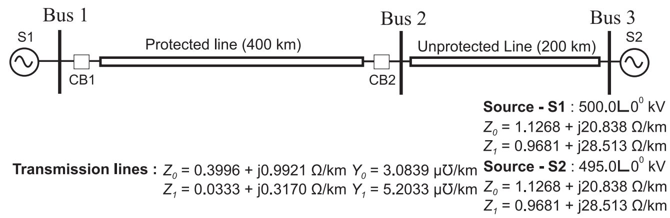

Fig. 2. Power system model.

The simulation time step of the RTDS is Δt=50 μs. In this case, the sampling frequency used in this paper is f_s=20 kHz. Therefore, the frequency spectrum of the wavelet coefficients at the first scale falls into the range $[5, 10]$ kHz [15]. As a consequence, the wavelet coefficients at the first scale are well-suitable for a fast detection of the highest frequency components of the fault-induced transients [13]. In addition, the real-time computation of the wavelet coefficients by using only the first scale reduces the simulator efforts by comparing with applications in which various wavelet decompositions are required.

According to [16], the effectiveness of the wavelet analysis is largely influenced by the choice of the mother wavelet. However, the wavelet Daubechies 4 (db4) provides an accurate detection of the fast transients in power systems [5]. The four coefficients of the db4 filters provide a fast computation of the wavelet coefficients, which is an excellent feature for real-time applications [13].

The MODWT is a variant of the DWT. Both of them use low- and high-pass filters to divide the frequency-band of the input signal into low- and high-frequency components at various scales. However, in contrast to the DWT, there is no down-sampling process in MODWT [15]. As a consequence, the wavelet coefficient computation of the MODWT requires more computational effort. However, the MODWT provides twice the amount of coefficients to be analyzed in real-time (faster real-time analysis).

The computationally efficient pyramid algorithm of the MODWT can be easily adapted for real-time computation of the wavelet coefficients [13]. If the samples of the signal are obtained in real-time, the wavelet coefficient soon after each sampling process is given by

$$w(k) = \sum_{l=1}^{L} h(l)x(k+l-L), \tag{1}$$

since $\exists\{x(k\text{-}L\text{+}1),...,x(k\text{-}1),x(k)\}$; w are the wavelet coefficients of a signal x; h are the coefficients of the wavelet filter. The real-time simulator must be robust enough to solve the network equations and also compute the wavelet coefficients.

III. Real-Time Fault Detection and Location

In order to develop a wavelet-based method for fault detection and location, the transmission power system shown in Fig. 2 was modeled and simulated by using the RTDS. The system is composed of two 500 kV, 400 km long transmission lines: a protected line from bus 1 to bus 2 and an unprotected line between buses 2 and 3. The line parameters were obtained from actual transmission lines belonging to the Chesf utility, a Brazilian power system.

The real-time fault detection and location (Fig. 3) is composed of three modules:

- Fault-induced transient detection: The real-time detection of the fault-induced transients is independently accomplished in each line end.
- Internal Fault detection: After the fault-induced transient detection, the method in a specific bus needs information from another one in order to identify either internal or external faults.
- Fault location: taking into account the traveling wave velocity, the fault is located according to the fault-inception time at each line end.

When the proposed method is used at just one line end, only the fault-induced transients are detected.

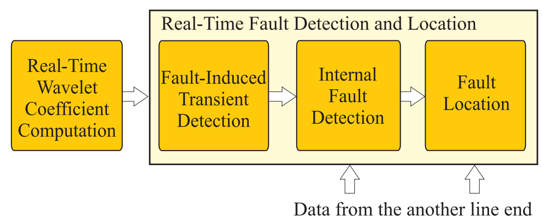

Fig. 3. Flowchart of the real-time fault detection and location.

A. *Fault-Induced Transient Detection in Real-Time*

During the steady-state system operation the voltages and currents are usually composed of a fundamental power frequency component, some harmonics, and noises with low and high frequency components. It is well known that power system noises present normal probability distribution [17].

At steady-state operation, the wavelet coefficients of the MODWT, at the first scale, are mainly influenced by the high frequency noises of the signals (from 5 to 10 kHz). After an extensive statistical analysis of actual oscillographic data from Chesf power system, it was verified that the wavelet coefficients can be approximated by a function with normal probability distribution with parameters given by the magnitude average μ and standard deviation σ. Similar features of the wavelet coefficients of the DWT were observed by [18].

Fig. 4 depicts the phase current of an actual oscillographic record without transient disturbances. The wavelet coefficients at the first scale and the related relative frequency histogram are also shown in Fig. 4. A normal probability density function with parameters given by the wavelet coefficient average and standard deviation was also obtained. The estimated density function and the density histogram match up quite well. In this case, the wavelet coefficients at the first scale are mainly due to the high frequency noises of the current and can be approximated by a function with normal probability distribution.

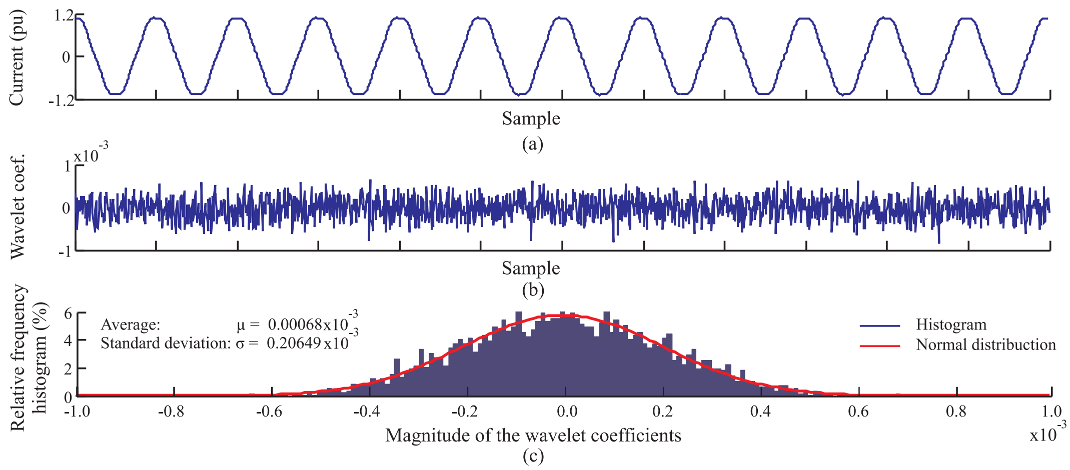

Fig. 4. High frequency noise analysis during steady-state operation: (a) phase current; (b) wavelet coefficients at the first scale; (c) density histogram of the wavelet coefficients.

According to the normal probability distribution function, about 99.73% of the wavelet coefficient values fall into the range [μ-3σ, μ+3σ]. During steady-state operation, all wavelet coefficients of a signal (voltage or current) are expected to be inside the range [W_1, W_2]=[μ-4σ, μ+4σ] (steady-state thresholds).

For each phase voltage and current, both W_1 and W_2 are computed in real-time considering the wavelet coefficients in the last cycle. The wavelet coefficient at the current simulation time step must present a value within the steady-state thresholds, i.e.: $w(k)\in[W_1, W_2]$.

When a line fault occurs, such as a fault due to an insulator flashover or fallen conductor, the abrupt change in voltage at the point of the fault generates a high frequency electromagnetic impulse called traveling wave which propagates along the line in both directions away from the fault point at speeds close to light velocity. As a consequence, fault-induced transients with low and high frequency components can be observed at each line end at a specific time after the fault inception. These transients can be properly detected by using the wavelet coefficients of voltages and currents: the wavelet coefficients regarding the fault-induced transients are higher than the ones related to steady-state.

Fig. 5 depicts the phase A voltage and current (v_A and i_A) at fault location, bus 1, and bus 2 (half cycle), regarding an AG fault with r_f=1 Ω, θ_f=90^o, and d_f=45 km from bus 1, simulated in real-time at the protected line of the power system shown in Fig. 2. The wavelet coefficients of the voltages and currents at buses 1 and 2 were also computed in real-time (Fig. 5).

According to Fig. 5, k_f is the sample related to the fault inception time. However, due to the traveling wave propagating time, the fault-induced transients at buses 1 and 2 were detected at samples k_{f1} and k_{f2}, respectively. The wavelet coefficients regarding these transients usually present very high values, mainly at k_{f1} and k_{f2} samples. Taking the wavelet coefficients at steady-state as reference, a fast increasing (or decreasing) of the wavelet coefficients at least in one of the voltages and currents allows the fault-induced transient detection in real-time. In this case, the wavelet coefficient of a specific signal at the current simulation time step must present a value outside the steady-state thresholds.

B. Fault Detection

Fig. 6 depicts a protected line with both internal and external faults. The monitored currents at each line end are taken as reference to be flowing into the protected line. In case of an internal fault (Fig. 6(a)), the traveling waves before any reflection and refraction propagate against the monitored current directions. As a consequence, the first wavelet coefficient peak of a current at both line ends presents the same polarities. With regard to external faults (Figs. 6(b) and (c)), the first wavelet coefficient peak of a current at both line ends presents opposite polarities to each other.

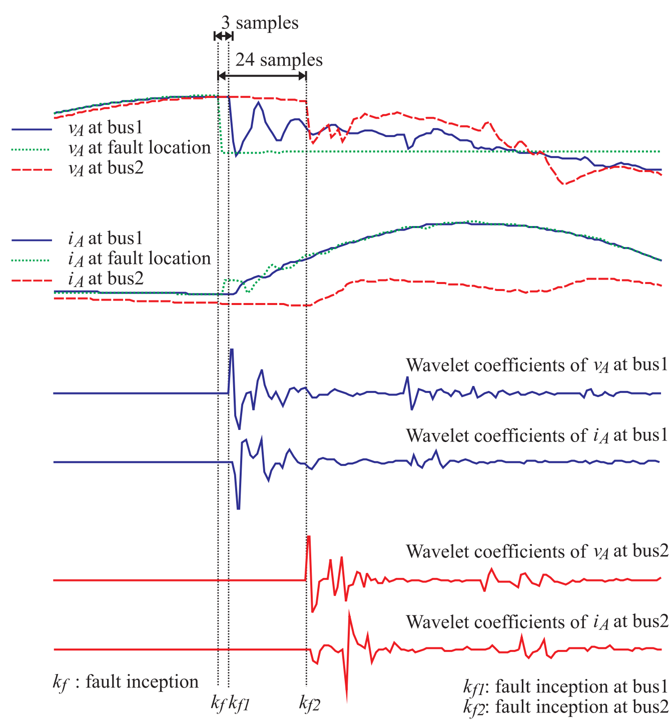

Fig. 5. Fault-induced transients of an internal fault detected by using the wavelet coefficients of the MODWT.

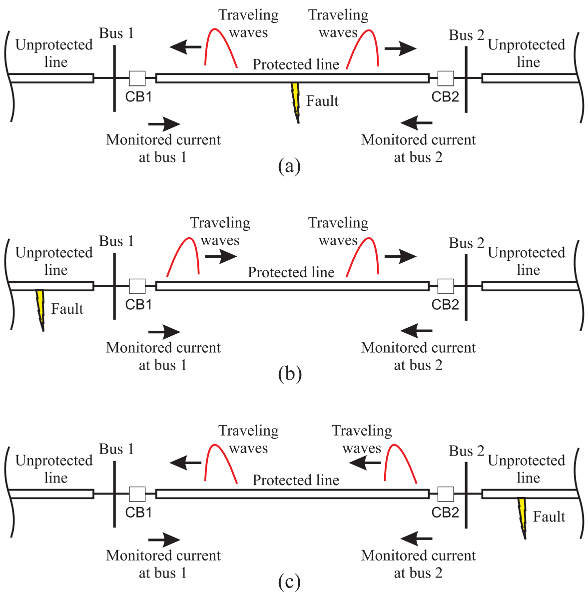

Fig. 6. Traveling waves and monitored current polarities: (a) inside fault; (b) left outside fault; (c) right outside fault.

When a fault is within the protected line and it is not in the middle of the line, fault-induced transients will be detected at distinct times at line terminals (Fig. 5). When these transients are detected at one of the line ends, a communication link between the buses is used in order to send information to another one. In this paper, both the traveling wave propagation time to cross the line and the communication time between the buses are taken as the same (Δk samples).

After both the fault-induced transient detection and communication between buses, the fault is taken as within the protected line whether the first wavelet coefficient peak of a specific current at both line ends present the same polarities. For instance, in Fig. 5, the wavelet coefficient peak of phase A current decreases at fault inception time at each line end.

Fig. 7 depicts the phase A voltage and current (v_A and i_A) at bus 1, bus 2, and fault location (half cycle), regarding an AG fault with r_f=14.9 Ω, θ_f=98.9^o, and d_f=70 km from bus 3, simulated in real-time on unprotected line of the power system shown in Fig. 2. The wavelet coefficients of these signals at buses 1 and 2 were also computed in real-time and shown in Fig. 7.

According to Fig. 7, the first wavelet coefficient peak of i_A at both line ends presented opposite polarities. In addition, the difference between the samples related to the fault-inception time at each line end is equivalent to the traveling wave propagation time to cross the line ($|k_{f1}$-$k_{f2}|\approx\Delta k$).

C. Real-Time Fault Location

How to define the velocity of the travelling wave correctly is critical to the accuracy of fault location methods based on fault-induced transient or travelling wave analysis. Most of fault location schemes consider the propagation velocity of travelling waves as the velocity of light. However, it is well-known that on multi-conductor transmission lines the travelling waves propagate with different velocities in different modes [19].

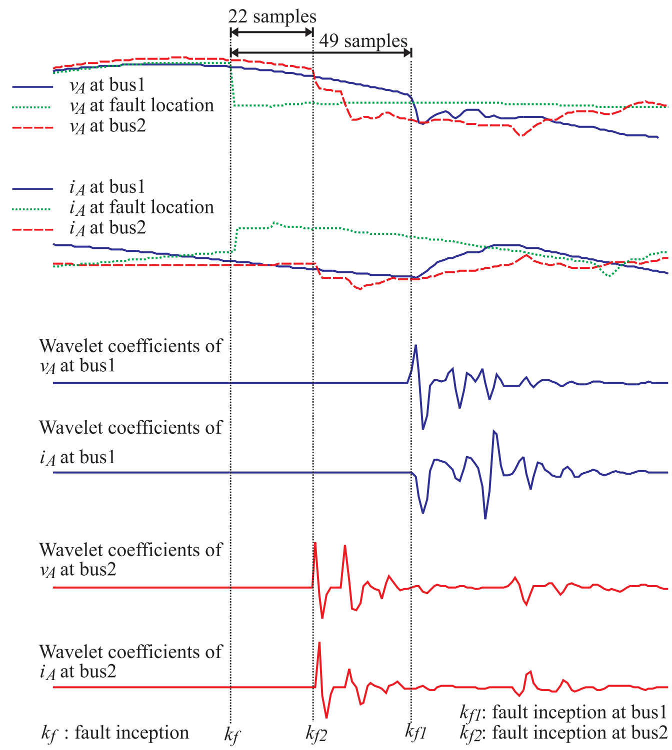

Fig. 7. Fault-induced transients of an external fault detected by using the wavelet coefficients of the MODWT.

The propagation velocity of the travelling wave was computed by using the distributed parameter model of a long transmission line. In this paper, by using the distributed parameters shown in Fig. 2, the propagation velocity of the travelling wave was taken as 98% of the velocity of light. By using this velocity, the waves propagate ΔL km in one time step of 50 μs. Therefore, each sample from the fault inception time (sample k_f) to the fault inception time at monitored bus (samples k_{f1} or k_{f2}) represents a fault away $\Delta L\approx$15 km.

According to Fig. 5, at bus 1, the fault-induced transients could be detected 3 samples after the fault inception time (k_{f1}-k_f=3: fault located about 45 km away from bus 1). On the other hand, at bus 2, the fault-induced transients could be detected 24 samples after the fault inception time (k_{f2}-k_f=24: fault located about 360 km away from bus 1). This fault was simulated on the protected line, 45 and 355 km away from buses 1 and 2, respectively.

Taking into account the simulation time step Δt=50 μs, the sample amount equivalent to the traveling wave propagation time to cross a 400 km transmission line is 27 samples (Δk=27 samples). According to Fig. 7, at bus 2, the fault-induced transients could be detected 22 samples after the fault inception time (k_{f2}-k_f=22: fault located about 330 km away from bus 2). On the other hand, at bus 1, the fault-induced transients could be detected 49 samples after the fault inception time (k_{f1}-k_f=49: fault located about 735 km away from bus 1). This fault was simulated upon an unprotected line, 330 and 730 km away from buses 2 and 1, respectively. Beyond the polarities of the first wavelet coefficient peak of the currents in both buses, the comparison between the fault location estimation of both buses can also indicate whether a fault is internal the protected line.

According to [14], [13], the sample regarding the fault-induced transients at monitored buses (k_{f1} and k_{f2}) can be faster and accurately detected by means of the wavelet coefficient analysis of the MODWT. However, the sample regarding the fault inception upon the transmission line k_f can not be identified by means of voltage and current analysis at a specific bus. Fortunately, the fault location can be estimated through the samples k_{f1} and k_{f2}, as follows

$$d_{ij} = \frac{L - \Delta t(k_{fj} - k_{fi}) * v}{2}, \quad (2)$$

where d_{ij} is the fault location estimation at bus i by using additional information from bus j; L is the line length; v is the propagation velocity of the traveling wave; k_{fi} and k_{fj} are the samples regarding the fault-induced transient detection at buses i and j, respectively. In this paper, v=0.98c, where c is the velocity of the light.

By using Eq. 2 with v=0.98c, the fault location estimation regarding the internal fault shown in Fig. 5 would be d_{12}=45.65 km from bus 1 and d_{21}=354.35 km from bus 2. In this case, an internal fault is identified. With regard to the external fault shown in Fig. 7, the fault location estimation would be d_{12}=398.45 km from bus 1 and d_{21}=1.55 km from bus 2. In this case, an external fault is identified. In this paper, an external fault is identified when $d_{ij} \geqslant L$-ΔL and $d_{ji} \leqslant \Delta L$, or vice-versa. In addition, transients due to a switching operation either on protected line terminals or other power system equipment away from the protected line can be detected as external faults.

In this paper, a communication link between the buses is used in order to detect an internal fault and estimate the fault location in each bus. The communication delay between the buses was taken as Δk=27 samples. When the fault-induced transients are detected at bus i, information regarding the polarities of the wavelet coefficients of the currents and the samples in which these transients were detected (k_{fi}) are sent to bus j. Therefore, the fault detection and location at bus j is carried out at sample k_{lj}=k_{fi}+Δk. As analogy, the fault detection and location at bus i is carried out when information from bus j were received, at sample k_{li}=k_{fj}+Δk. Therefore, the bus further from the fault will detect and locate the fault faster.

IV. Proposed Method Performance Evaluation

The transmission power system shown in Fig. 2 was modeled and simulated by using the RTDS. The proposed method was also modeled by using the RTDS at two distinctive power system points (buses 1 and 2) in order to detect and locate internal faults upon a protected line (Fig. 8). The transducers were modeled with typical parameters.

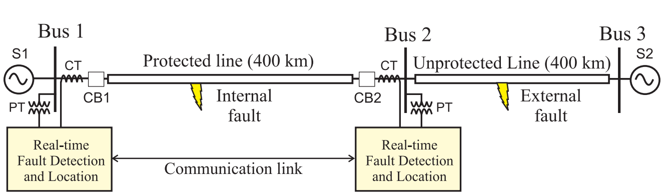

Fig. 8. Power system model with the proposed fault detection and location method.

In order to evaluate the performance of the wavelet-based method for real-time fault detection and location, a total of 1000 faults on protected line was simulated in real-time, each one with random values of fault resistance $r_f \in \{0,\ 50\}$ Ω, fault inception angle $\theta_f \in \{0^o,\ 180^o\}$, and fault location $d_f \in \{15,\ 385\}$ km from bus 1. With regard to the fault type, 100 AG, BG, CG, AB, BC, AC, ABG, BCG, ACG, and ABC faults were simulated. The fault-clearing time in each simulation was about 75 ms (4.5 cycles of 60 Hz).

The fault detection and location method was performed with both MODWT and DWT. The transients regarding the fault inception time at each line end were identified with a mean error of one sample (50 μs) by means of the real-time MODWT and about two samples with the real-time DWT, due to the down-sampling process to compute the wavelet coefficients. Therefore, the faults were detected faster by using the MODWT. With regard to the fault detection, in both MODWT- and DWT-based methods, all faults were detected as internal faults after the communication of the fault locators.

With regard to the fault location, the MODWT-based method provided a mean error of 0.65% and 0.63% at buses 1 and 2, respectively. By using the DWT-based method, mean errors of 1.05 and 1.02% were obtained at buses 1 and 2, respectively. The mean error at fault location for all types of faults is summarized in Tab. I. The fault location is not influenced by the type of fault and provides better performance with the MODWT.

A total of 1000 faults on unprotected line was also simulated in real-time, each one with random values of fault resistance $r_f \in \{0,\ 50\}$ Ω, fault inception angle $\theta_f \in \{0^o,\ 180^o\}$, and fault location $d_f \in \{15,\ 385\}$ km from bus 2. With regard to the fault type, 100 AG, BG, CG, AB, BC, AC, ABG, BCG, ACG, and ABC faults were simulated. The fault-clearing time in each simulation was about 75 ms (4.5 cycles of 60 Hz). In all cases, the fault-induced transients were successfully detected and the faults were detected as external faults by using both MODWT and DWT.

In order to improve the obtained results, a sensitivity analysis of the effectiveness of the proposed wavelet-based fault detection and location scheme with reference to different mother wavelets have been performing and will be addressed in future works.

TABLE I
Performance evaluation of both MODWT- and DWT-based methods.

Type of fault	Amount of simulations	Mean error (%)			
		Bus 1		Bus 2	
		MODWT	DWT	MODWT	DWT
AG	100	0.6452	1.0656	0.6143	1.0556
BG	100	0.6535	1.0539	0.6336	1.0399
CG	100	0.6047	1.0470	0.6570	1.0453
AB	100	0.6691	1.0730	0.6388	0.9686
BC	100	0.7002	1.1040	0.6590	1.0451
AC	100	0.7439	1.0722	0.5866	0.9264
ABG	100	0.7147	1.0802	0.6836	1.0098
BCG	100	0.5976	1.0581	0.5509	1.0605
ACG	100	0.6032	1.9443	0.6139	1.0094
ABC	100	0.6098	1.0004	0.6221	1.0373

The proposed fault location scheme can provide good performance with high sampling frequency. However, good results were obtained on real-time simulation of the RTDS by using a sampling frequency of 20 kHz (simulation time step of 50 μs). Nowadays, this sampling frequency can be used by high-speed protective relays. The proposed MODWT-based analysis will be further implemented into a new directional relaying scheme in order to design a reliable method for high-speed fault clearance in protection systems.

V. Conclusions

The real-time fault detection and location based on the wavelet coefficient analysis was very fast, performing both the high-speed fault detection and good fault location. this can make it a promising candidate for a protective relaying algorithm. In addition, the method seems to be little dependent on the conditions that would affect most of the other algorithms, such as line parameters and fault parameters (resistance, location, inception angle, and type).

The real-time fault detection and location method was performed with both the discrete wavelet transform and the maximal overlap discrete wavelet transform. The fault-induced transients were detected faster and the faults were located accurately by using the maximal overlap discrete wavelet transform.

Taking into account the sampling frequency of 20 kHz (value near the typical digital fault recorders), the obtained fault location accuracy (mean error of about 0.63% with the maximal overlap discrete wavelet transform) is quite remarkable.

References

[1] G. W. Swift, "The spectra of fault-induced transients," *IEEE Transactions on Power Apparatus and Systems*, vol. PAS-98, no. 3, pp. 940–947, May 1979.

[2] A. T. Johns, R. K. Aggarwal, and Z. Q. Bo, "Non-unit protection technique for ehv transmission systems based on fault-generated noise, part 1: Signal measurement," *IEE Proc. Gener. Transm. Distrib.*, vol. 141, no. 2, pp. 133–140, March 1994.

[3] Z. Bo, M. Redfern, and G. Weller, "Positional protection of transmission line using fault generated high frequency transient signals," *IEEE Transactions on Power Delivery*, vol. 15, no. 3, pp. 888 –894, Jul. 2000.

[4] S. Santoso, E. J. Powers, W. M. Grady, and P. Hofmann, "Power quality assessment via wavelet transform analysis," *IEEE Transactions on Power Delivery*, vol. 11, no. 2, pp. 924–930, April 1996.

[5] M. H. J. Bollen and I. Y.-H. Gu, *Signal Processing of Power Quality Disturbances*. New York, USA: IEEE, 2006.

[6] W. A. Wikinson and M. D. Cox, "Discrete wavelet analysis of power system transients," *IEEE Transactions on Power Systems*, vol. 11, no. 4, pp. 2038–2044, Nov 1996.

[7] S. A. Probert and Y. H. Song, "Detection and classification of high frequency transients using wavelet analysis," *Proc. 2002 IEEE Power Engineering Society Summer Meeting*, vol. 2, pp. 801–806, Chicago, USA, July 2002.

[8] F. B. Costa, B. A. Souza, and N. S. D. Brito, "Detection and classification of transient disturbances in power systems," *IEEJ Trans. PE*, pp. 910–916, Oct 2010.

[9] O. A. S. Youssef, "Fault classification based on wavelet transforms," *Transmission and Distribution Conference and Exposition*, vol. 1, pp. 531–536, Nov 2001.

[10] K. M. Silva, B. A. Souza, and N. S. D. Brito, "Fault detection and classification in transmission lines based on wavelet transform and ann," *IEEE Transactions on Power Delivery*, vol. 21, no. 4, pp. 2058–2063, Oct 2006.

[11] D.-J. Zhang, Q. H. Wu, Z. Q. Bo, and B. Caunce, "Transient positional protection of transmission lines using complex wavelets analysis," *IEEE TRANSACTIONS ON POWER DELIVERY*, vol. 18, no. 3, pp. 705–710, jul. 2003.

[12] S. P. Valsan and K. Swarup, "Wavelet transform based digital protection for transmission lines," *International Journal of Electrical Power & Energy Systems*, vol. 31, no. 7-8, pp. 379–388, 2009.

[13] F. B. Costa, B. A. Souza, and N. S. D. Brito, "Real-time detection of fault-induced transients in transmission lines," *IET Electronics Letters*, pp. 753–755, May 2010.

[14] F. B. Costa, "Uma técnica de diagnóstico em tempo real de distúrbios transitórios baseada na transformada wavelet para uso em registradores digitais de perturbação," Ph.D. dissertation, Federal University of Campina Grande, Campina Grande, Brazil, 2010.

[15] D. B. Percival and A. T. Walden, *Wevelet Methods for Time Series Analysis*. New York, USA: Cambridge University Press., 2000.

[16] L. Peretto, R. Sasdelli, and R. Tinarelli, "On uncertainty in wavelet-based signal analysis," *Instrumentation and Measurement, IEEE Transactions on*, vol. 54, no. 4, pp. 1593 – 1599, 2005.

[17] W. D. Stevenson JR. and J. J. Grainger, *Power System Analysis*. New York, USA: McGraw-Hill, 1994.

[18] A. C. Parsons, W. M. grady, and E. J. Powers, "A wavelet-based procedure for automatically determining the beginning and end of transmission system voltage sags," *IEEE Power Engineering Society 1999 Winter Meeting*, vol. 2, pp. 1310–1315, Feb. 1999.

[19] J. D. Glover and M. S. Sarma, *Power System Analysis and Design*. New York: Thomson-Engineering publisher, 2002.

F. B. Costa received his BS, MS, and PhD in Electrical Engineering from Federal University of Campina Grande (UFCG), Brazil, in 2005, 2006, and 2010, respectively. He works currently as a professor at Federal University of Rio Grande do Norte - School of Science and Technology, Brazil. He received an honorable mention from the 2010 Brazilian Award of Engineering for his Ph.D. dissertation on fault and power quality problems. His research interest are electromagnetic transients, power quality, fault diagnosis, and power system protection.

B. A. Souza received his PhD in Electrical Engineering from Federal University of Paraíba, Brazil, in 1995. He currently works as a professor at the Department of Electrical Engineering of Federal University of Campina Grande, Brazil. His main research activities are on optimization methods applied to power systems, electromagnetic transients, power quality and fault diagnostic.